Post-Fault Operation of an Asymmetrical Six-phase Induction Machine with Single and Two Isolated Neutral Points

Hand Seng Che, Mario J. Duran, Emil Levi, *Fellow, IEEE,* Martin Jones, Wooi-Ping Hew, *Member, IEEE,*
Nasrudin Abd. Rahim, *Senior Member, IEEE*

Abstract – **The paper presents a study of post-fault control for an asymmetrical six-phase induction machine with single and two isolated neutral points, during single open-phase fault. Post-fault control is based on the normal decoupling (Clarke) transformation, so that reconfiguration of the controller is minimised. Effect of the single open-phase fault on the machine equations under this control structure is discussed. Different modes of post-fault operation are analysed and are further compared in terms of the achievable torque and stator winding losses. Validity of the analysis is verified using experimental results obtained from a six-phase induction motor drive prototype.**

*Index Terms –***Fault-tolerant operation, multiphase machines, variable-speed drives.**

I. Introduction

One important advantage of a multiphase machine over its three-phase counterpart is its higher fault-tolerance [1]. Hence, fault-tolerant operation and control are important research topics in this area. Although fault tolerance can be achieved via special machine design [2]–[6] and the use of application-specific converter topologies [7]–[10], the majority of studies [11]–[26] focus on the post-fault control methods for *n*-phase machines driven by an *n*-leg voltage source converter (VSC), since this is the most common topology in practice. The discussion here follows this common trend, assuming star-connected stator windings.

Among multiphase machine, machines with multiple three-phase windings, such as six-, nine-, and twelve-phase machines, are often considered for various applications. Compared with multiphase machine with prime phase numbers, machines with multiple three-phase windings can benefit from the well-established three-phase technology. Due to the existence of the multiple winding sets, the machine can be configured with single or multiple neutral points. Fig. 1 shows the connections of stator windings for an asymmetrical six-phase machine with single and two neutral
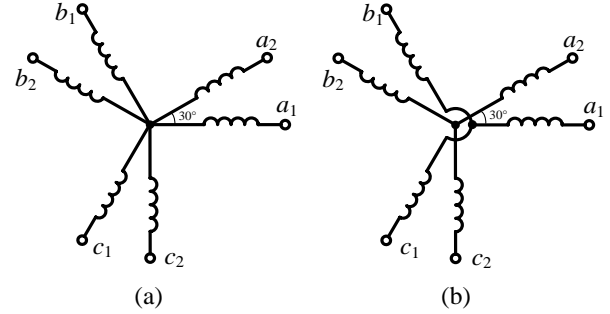

Fig. 1. Stator winding magnetic axes in an asymmetrical six-phase machine with (a) single and (b) two neutral points (positive direction is clockwise).

points. Each possibility has its own merits. For instance, configuration of a six-phase machine with two isolated neutrals prevents the flow of zero-sequence currents and reduces the required number of current controllers from five to four. In addition, it provides isolation between the two windings and allows better dc-bus voltage utilisation. On the other hand, single isolated neutral point connection gives five instead of four degrees of freedoms, which provides better means for fault-tolerant operation. However, it requires additional controller for regulating the zero-sequence current. Hence, in the literature, discussion on healthy operation of six-phase machines is usually based on two isolated neutrals, while fault-tolerant control studies are typically based on single neutral connection [12], [13], [20], [27].

The simplest post-fault strategy for multiphase machines with multiple three-phase windings is to disable the whole three-phase winding containing the faulty phase [1]. Such operation has been reported in [28] for aircraft steering control and in [29] for an elevator application. This approach is addressed as 'single VSC' operation hereafter, for the specific case of a six-phase drive. Instead of disabling the whole three-phase winding, which causes significant reduction in achievable power/torque, better performance can be obtained via suitable post-fault control. Such control has been discussed in [12], [13], [20], [27], with the six-phase machine configured with single isolated neutral. Discussion on fault-tolerant control of a six-phase machine with two isolated neutrals is available in [22], [23], but is accompanied with only simulation studies and very limited experimental verification. A more complete study for two-neutral configuration was reported in [24], where suitable post-fault control strategy was shown to give better efficiency than 'single VSC' operation. However, the control uses PI controllers to regulate ac references, which results in poor

performance. So far, a comprehensive discussion covering both configurations has not been reported.

This work aims to provide a unified discussion on the post-fault control of a six-phase induction machine during single open-phase fault, by considering both single and two isolated neutrals configurations. The focus is on asymmetrical six-phase induction machine (with two three-phase windings spatially displaced by 30 degrees) with distributed windings. The discussion presented here differs from previous works in the following aspects:

1) The post-fault control uses normal (i.e. not a reduced order) decoupling transformation, which allows the use of the same controller structure as in the healthy operation. Such control has been discussed in [16], [21], but not for an asymmetrical six-phase machine.

2) A unified analysis of post-fault control of the six-phase machine, considering both single and two isolated neutrals, is presented. Results show that the same controller structure is applicable for both configurations, requiring only minor alterations. Quantitative comparisons between the two, in terms of the achievable torque and stator winding losses under different modes of post-fault control, are presented as well.

The paper is organized as follows. Section II describes the machine equations and control structure of a healthy six-phase induction machine. Section III shows the influence of fault on machine equations when the same decoupling transformation is maintained. Section IV discusses the derivation of current references for different modes of post-fault operation. Derating of the machine is also detailed here. Next, Section V discusses the current controllers used, and the modifications for post-fault operation. Experimental verification of the analysis, based on a prototype asymmetrical six-phase induction motor drive, is presented in Section VI. Finally, concluding remarks are given in Section VII.

II. MACHINE EQUATIONS AND CONTROL STRUCTURE FOR HEALTHY MACHINE

Control of a healthy asymmetrical six-phase induction machine is usually based on the vector space decomposition (VSD) model. Using the VSD model, the machine phase variables $[f_k]$ are related to the new variables $[f_{\alpha\beta xy}]$ via decoupling transformation $[T_6]$ (f represents arbitrary machine variables (voltage v, current i or flux ψ)):

$$[f_{\alpha\beta xy}] = [T_6] \cdot [f_k] \tag{1}$$

where

$$[f_k] = \begin{bmatrix} f_{a1} & f_{b1} & f_{c1} & f_{a2} & f_{b2} & f_{c2} \end{bmatrix}^T$$
$$[f_{\alpha\beta xy}] = \begin{bmatrix} f_\alpha & f_\beta & f_x & f_y & f_{0+} & f_{0-} \end{bmatrix}^T \tag{2}$$

$$[T_6] = \frac{1}{\sqrt{3}} \begin{array}{c} \alpha \\ \beta \\ x \\ y \\ 0+ \\ 0- \end{array} \begin{bmatrix} 1 & -\frac{1}{2} & -\frac{1}{2} & \frac{\sqrt{3}}{2} & -\frac{\sqrt{3}}{2} & 0 \\ 0 & \frac{\sqrt{3}}{2} & -\frac{\sqrt{3}}{2} & \frac{1}{2} & \frac{1}{2} & -1 \\ 1 & -\frac{1}{2} & -\frac{1}{2} & -\frac{\sqrt{3}}{2} & \frac{\sqrt{3}}{2} & 0 \\ 0 & -\frac{\sqrt{3}}{2} & \frac{\sqrt{3}}{2} & \frac{1}{2} & \frac{1}{2} & -1 \\ 1 & 1 & 1 & 0 & 0 & 0 \\ 0 & 0 & 0 & 1 & 1 & 1 \end{bmatrix} \tag{3}$$
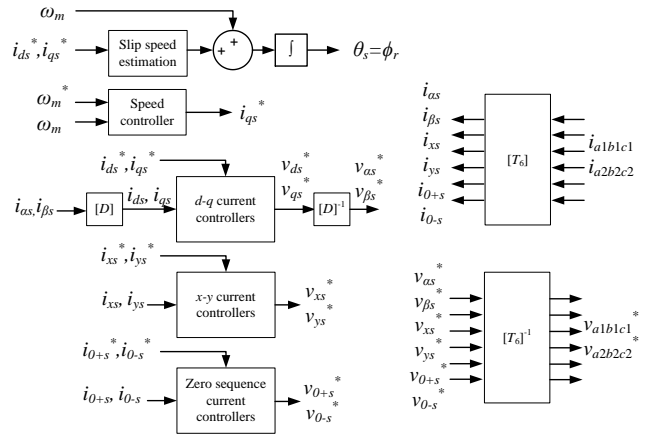

Fig. 2. Control structure for IRFOC of a six-phase induction machine.

For an induction machine with sinusoidally distributed windings and negligible mutual leakage inductance between the three-phase windings, the machine stator equations in the stationary common reference frame are:

$$v_{\alpha s} = (R_s + L_s \cdot \tfrac{d}{dt}) i_{\alpha s} + M \cdot \tfrac{d}{dt} i_{\alpha r}$$
$$v_{\beta s} = (R_s + L_s \cdot \tfrac{d}{dt}) i_{\beta s} + M \cdot \tfrac{d}{dt} i_{\beta r}$$
$$v_{xs} = (R_s + L_{ls} \tfrac{d}{dt}) i_{xs}$$
$$v_{ys} = (R_s + L_{ls} \tfrac{d}{dt}) i_{ys} \tag{4}$$
$$v_{0+s} = (R_s + L_{ls} \tfrac{d}{dt}) i_{0+s}$$
$$v_{0-s} = (R_s + L_{ls} \tfrac{d}{dt}) i_{0-s}$$

while the rotor equations are

$$0 = (R_r + L_r \tfrac{d}{dt}) i_{\alpha r} + \omega_r L_r i_{\beta r} + M \tfrac{d}{dt} i_{\alpha s} + \omega_r M i_{\beta s}$$
$$0 = (R_r + L_r \tfrac{d}{dt}) i_{\beta r} - \omega_r L_r i_{\alpha r} + M \tfrac{d}{dt} i_{\beta s} - \omega_r M i_{\alpha s} \tag{5}$$

where $L_s = L_{ls} + 3L_{ms}$, $L_r = L_{lr} + 3L_{ms}$, $M = 3L_{ms}$ and ω_r is the rotor electrical speed ($\omega_r = p\omega_r$, p being the pole pair number). Subscripts s and r denote stator and rotor variables, respectively.

For a machine with sinusoidally distributed windings, only the α-β components contribute to flux and torque production. As in the three-phase case, rotational transformation $[D]$ can be used to transform α-β components into the general synchronous reference frame d-q components (θ_s is the angle of transformation, which will subsequently be equal to the rotor flux position):

$$[D] = \begin{bmatrix} \cos\theta_s & \sin\theta_s \\ -\sin\theta_s & \cos\theta_s \end{bmatrix} \tag{6}$$

Indirect rotor flux oriented control (IRFOC) is achieved by using $\theta_s = \phi_r$, where rotor flux angle ϕ_r is obtained from measured rotor position (or speed ω_m) and reference d-q stator currents. The controller's structure for IRFOC of a six-phase induction machine is shown in Fig. 2. References for i_{xs}, i_{ys}, i_{0-s} and i_{0-s} are normally set to zero, to minimise stator copper losses.

Regardless of the neutral point connection (single or two isolated neutrals), the same controller structure can be used, with a difference that for the two isolated neutrals the zero-sequence current controllers are, since i_{0+s} and i_{0-s} cannot flow, disabled by setting $v_{0+s}{}^* = v_{0-s}{}^* = 0$.

III.   MACHINE EQUATIONS FOR POST-FAULT OPERATION

The fault considered here is an "open-phase fault" that open-circuits the connection between one of the VSC's legs and the machine. It is assumed that the machine's phase winding is not damaged during the fault.

When an open-phase fault occurs, the corresponding phase current becomes zero, and the machine loses one degree of freedom. Some of the previous works [11]–[14] approached the problem by utilizing new reduced-order decoupling transformations to reflect the loss of one degree of freedom. However, the machine equations obtained from the reduced-order transformation have different machine parameters and substantial reconfiguration of the controller is required.

To minimize changes to the control, it appears to be better to retain the same decoupling transformation ($[T_6]$ in this case), so that the same controller structure can be used. Such control has been presented for a seven-phase PM machine in [16], and later extended for induction machines with odd numbers of phases in [21]. However, discussions in [16], [21] only cover the effect of fault on machine's MMF and do not address the changes in machine equations as a whole, which is done here next.

A.   Effect of Fault on Machine Equations

If the transformation of machine equations from phase variables to the stationary reference frame variables is analyzed, it is obvious that (4)-(5) need not be changed because the machine is not physically affected by the fault. The main effect of the open-phase fault is on the currents, where α-β-x-y-$0+$-$0-$ components are no longer mutually independent due to the loss of one degree of freedom. Hence, it is necessary to find the currents' relationship during fault and the subsequent effects on the machine equations.

For the purpose of discussion, it is assumed that open circuit fault occurs in phase-$c2$, so that i_{c2} is zero. The α, x and $0+$ currents, which do not contain phase-$c2$ term, remain unaffected by this fault. However, the equations for β, y and $0-$ currents are affected and they become:

$$i_{\beta s} = \frac{1}{\sqrt{3}}\left(\frac{\sqrt{3}}{2}i_{b1s} - \frac{\sqrt{3}}{2}i_{c1s} + \frac{1}{2}i_{a2s} + \frac{1}{2}i_{b2s}\right)$$

$$i_{ys} = \frac{1}{\sqrt{3}}\left(-\frac{\sqrt{3}}{2}i_{b1s} + \frac{\sqrt{3}}{2}i_{c1s} + \frac{1}{2}i_{a2s} + \frac{1}{2}i_{b2s}\right) \qquad (7)$$

$$i_{0-s} = \frac{1}{\sqrt{3}}\left(i_{a2s} + i_{b2s}\right)$$

These are the general expressions that are valid regardless of how the neutral points are configured.

For *two isolated neutrals*, the phase currents in each three-phase winding must sum to zero ($i_{0+s} = i_{0-s} = 0$). Hence, when $i_{c2s} = 0$, $i_{a2s} = -i_{b2s}$, and (7) simplifies to

$$i_{ys} = -i_{\beta s}$$

$$i_{0-s} = 0 \qquad (8)$$

Since $i_{0+s} = i_{0-s} = 0$ and $i_{\beta s}$ is now directly related to i_{ys}, the machine practically has only three degrees of freedom (α, β and x) during the single open-phase fault.

Note that there are no changes in the equations for α-β and x components (4). Also, the zero-sequence voltage equations in (4) can be discarded because $i_{0+s} = i_{0-s} = 0$. However, as i_{ys}

and $i_{\beta s}$ are no longer mutually independent, the stator y-axis equation is now:

$$v_{ys} = \left(R_s + L_{ls}\frac{d}{dt}\right)\cdot i_{ys} = -\left(R_s + L_{ls}\frac{d}{dt}\right)\cdot i_{\beta s} \qquad (9)$$

If the machine is configured with *single neutral point*, the following relation can be derived:

$$i_{0-s} = \frac{1}{\sqrt{3}}\left(i_{a2s} + i_{b2s}\right) = i_{\beta s} + i_{ys}$$

$$i_{0+s} = -i_{0-s} \qquad (10)$$

The main difference compared with the two-neutral point case is that i_{ys} is now an independent variable, giving the system four degrees of freedom (α, β, x and y).

Machine equations for α-β and x-y components remain the same as in (4) and (5). Due to the single neutral point connection, zero-sequence currents can now flow. They are, however, dependent on $i_{\beta s}$ and i_{ys} due to the fault, as shown in (10). As a result, the corresponding stator voltage equations are now:

$$v_{0+s} = (R_s + L_{ls}\frac{d}{dt})i_{0+s} = (R_s + L_{ls}\frac{d}{dt})(i_{\beta s} + i_{ys})$$

$$v_{0-s} = (R_s + L_{ls}\frac{d}{dt})i_{0-s} = -(R_s + L_{ls}\frac{d}{dt})(i_{\beta s} + i_{ys}) \qquad (11)$$

B.   Effect on Torque Equation

The post-fault torque equation can be obtained by considering the following phase variable equation:

$$T_e = p[i_{ks}]^T \cdot \frac{d}{d\theta_r}[L_{sr}]\cdot [i_{kr}] \qquad (12)$$

where θ_r is the rotor position angle and $[L_{sr}]$ is the rotor-to-stator inductance matrix.

Since the machine is physically the same, $[L_{sr}]$ is considered to be unaffected by the fault. This also implies that even though i_{c2s} cannot flow, voltage can still be induced in phase-$c2$ (in a form of back emf) due to the variation in stator and rotor currents.

By transforming (12), the torque equation during fault results in the same form as for the healthy machine.

$$T_e = pM\left(i_{\beta r}\cdot i_{\alpha s} - i_{\alpha r}\cdot i_{\beta s}\right) \qquad (13)$$

This is actually a similar conclusion to the one in [16], [21].

C.   Conclusions on Post-fault Machine Equations

Three important conclusions can be drawn from the post-fault machine equations based on $[T_6]$:

i)   The α-β equations, which are responsible for flux and torque production, remain unchanged even after the fault. Hence, no modifications of machine parameters are required in the implementation of FOC, unlike in [11]–[14], where reduced-order transformations are used.

ii)   The y or zero-sequence components are no longer independent during fault, as shown by (8) and (10). For a healthy machine, these current components are usually controlled to zero for loss minimization. However, during the fault, an attempt to control them to zero will cause disruption in the α-β current regulation. Hence, the current references need to be adapted during fault.

iii)   The torque equation is not affected by the fault, as indicated in (13). Thus, for smooth torque during fault, the α-β stator current references should take the following form:

$$i_{\alpha s}^{\ *} = \left| I_{\alpha\beta} \right| \cos(\omega_s t)$$
$$i_{\beta s}^{\ *} = \left| I_{\alpha\beta} \right| \sin(\omega_s t) \tag{14}$$

Based on (14), the trajectory of the post-fault α-β stator current vector ($i_{\alpha\beta} = i_{\alpha s} + j i_{\beta s}$) should be circular, just like in the case of a healthy machine.

IV. POST-FAULT OPERATION

A. Derating Factor

If the faulted machine is to generate rated flux and torque, the phase currents will increase above their rated values. Prolonged operation with such higher-than-rated phase currents is hazardous as it may violate the thermal limit of the machine and power electronic converter. Hence, for continuous post-fault operation, the machine should be "derated", i.e. run below rated values. This is not a problem for applications like traction and offshore wind generation, where operation at rated power is not compulsory and the need for prolonged post-fault operation is highly likely.

To illustrate the amount of derating required, a variable termed "derating factor", a, is considered in the following discussion. The derating factor is the factor by which the flux and torque currents ($|I_{\alpha\beta}|$) need to be scaled down for derated operation. This variable is defined as the ratio of the post-fault α-β (or d-q) currents' magnitude to the pre-fault current magnitude (rated phase current rms is denoted with I_n):

$$a = \frac{\left| I_{\alpha\beta} \right|_{post\_fault}}{\left| I_{\alpha\beta} \right|_n} = \frac{\left| I_{dq} \right|_{post\_fault}}{\left| I_{dq} \right|_n} = \frac{\left| I_{dq} \right|_{post\_fault}}{\sqrt{6} I_n} \tag{15}$$

A derating factor of 1 implies that the machine is not derated and is producing rated flux and torque. For any value $a < 1$, the machine operates with lower-than-rated flux and torque current, and is considered to be derated. While α–β current magnitude is important in determining the flux and torque of the machine, it is however the phase current amplitude that needs to be limited. Thus, a "threshold derating factor", a_o, is defined here as the derating factor required to keep the maximum post-fault phase current equal to the rated value. The relation between maximum peak post-fault phase current and rated phase current is hence given by

$$a_o = a \frac{\sqrt{2} I_n}{\max(i_{phase\_post\_fault})} = \frac{\left| I_{dq} \right|_{post\_fault}}{\sqrt{3} \max(i_{phase\_post\_fault})} \tag{16}$$

Since the post-fault machine equations have identical form as in the pre-fault case, the torque equation can be expressed in terms of the d-q currents, assuming RFOC, as:

$$T_e = p \frac{M^2}{L_r} i_{ds} i_{qs} \tag{17}$$

When the fault happens, it may be necessary to derate the machine by reducing the i_{ds} and i_{qs}, to keep the maximum phase current within acceptable limits. If both i_{ds} and i_{qs} are scaled down by factors a_d and a_q respectively, the achievable torque in terms of rated torque is given by expression

$$T_{e\_post\_fault} = a_d a_q T_{en} \tag{18}$$

The achievable torque in derated operation depends on how i_{ds} and i_{qs} are scaled down. Here, it is suggested to keep i_{ds} at rated value, and only derate i_{qs} ($a_d = 1$ and $a_q < 1$) to keep the phase current amplitude at rated:

$$T_{e\_post\_fault} = a_q T_{en} \tag{19}$$

The influence of a_q on the overall reduction of the d-q current magnitude (which is also the derating factor, a) is given with

$$a = \sqrt{\frac{i_{dsn}^2 + a_q^2 \cdot i_{qsn}^2}{i_{dsn}^2 + i_{qsn}^2}} \tag{20}$$

The expressions in (19) and (20) indicate that the achievable torque during post-fault operation depends on the ratio i_{dsn}/i_{qsn}. For a special case of $i_{dsn}/i_{qsn} = 0$, applicable to a permanent magnet machine, the post-fault torque varies linearly with a. For an induction machine, the variation in torque is non-linear when the machine is derated, with a higher i_{dsn}/i_{qsn} ratio giving a more rapid reduction in achievable torque during derated operation. This will be confirmed later in the experimental results.

B. Modes of Operation

While the α-β (d-q) stator currents determine the flux and torque of the machine, the other current components provide additional degrees of freedom which define the mode of post-fault operation. For this purpose, the x-y currents are defined in the following general form:

$$i_{xs}^{\ *} = K_1 i_{\alpha s}^{\ *} + K_2 i_{\beta s}^{\ *}$$
$$i_{ys}^{\ *} = K_3 i_{\alpha s}^{\ *} + K_4 i_{\beta s}^{\ *} \tag{21}$$

The values of K_1, K_2, K_3 and K_4 can be chosen based on the desired modes of operation. In this paper, two different modes of operation are considered, i.e.:

1) Min Loss

Coefficients are selected to minimize the copper loss in the stator windings, which is defined as

$$P_{loss} = R_s \left(i_{a1s}^2 + i_{b1s}^2 + i_{c1s}^2 + i_{a2s}^2 + i_{b2s}^2 + i_{c2s}^2 \right)$$
$$= R_s \left(i_{\alpha s}^2 + i_{\beta s}^2 + i_{xs}^2 + i_{ys}^2 + i_{0+s}^2 + i_{0-s}^2 \right) \tag{22}$$

This is equivalent to minimizing ($i_{xs}^2 + i_{ys}^2 + i_{0+s}^2 + i_{0-s}^2$), i.e. the sum of squared current components that do not contribute to flux and torque production.

2) Max Torque

Coefficients are selected to produce the largest $|I_{\alpha\beta}|$ (hence the maximum torque) with the maximum phase current amplitude maintained at the rated value. This is equivalent to finding the coefficients that give the highest value of a_o.

The phase currents are related to the VSD variables via the inverse decoupling transformation $[T_6]^{-1}$:

$$[i_k]_s = [T_6]^{-1} \cdot [i_{\alpha\beta xy}]_s^T \tag{23}$$

The relationship between stator phase and α-β currents can be obtained by substituting (8) and (21) or (10) and (21), for two and single isolated neutral points, respectively, into (23) and rearranging the expression. Hence for *two isolated neutrals*:

$$\begin{bmatrix} i_{a1s}{}^* \\ i_{b1s}{}^* \\ i_{c1s}{}^* \\ i_{a2s}{}^* \\ i_{b2s}{}^* \end{bmatrix} = \frac{1}{\sqrt{3}} \begin{bmatrix} 1+K_1 & 0 \\ -\frac{1}{2}(1+K_1) & \sqrt{3}-\frac{1}{2}K_2 \\ -\frac{1}{2}(1+K_1) & -\sqrt{3}-\frac{1}{2}K_2 \\ \frac{\sqrt{3}}{2}(1-K_1) & -\frac{\sqrt{3}}{2}K_2 \\ -\frac{\sqrt{3}}{2}(1-K_1) & \frac{\sqrt{3}}{2}K_2 \end{bmatrix} \cdot \begin{bmatrix} i_{\alpha s}{}^* \\ i_{\beta s}{}^* \end{bmatrix} \quad (24)$$

while for a *single isolated neutral*:

$$\begin{bmatrix} i_{a1s}{}^* \\ i_{b1s}{}^* \\ i_{c1s}{}^* \\ i_{a2s}{}^* \\ i_{b2s}{}^* \end{bmatrix} = \frac{1}{\sqrt{3}} \begin{bmatrix} 1+K_1-K_3 & -1+K_2-K_4 \\ -\frac{1}{2}-\frac{K_1}{2}+\left(\frac{\sqrt{3}}{2}+1\right)K_3 & \frac{\sqrt{3}}{2}-1-\frac{K_2}{2}-\left(\frac{\sqrt{3}}{2}+1\right)K_4 \\ -\frac{1}{2}-\frac{K_1}{2}+\left(\frac{\sqrt{3}}{2}-1\right)K_3 & -\frac{\sqrt{3}}{2}-1-\frac{K_2}{2}+\left(\frac{\sqrt{3}}{2}-1\right)K_4 \\ \frac{\sqrt{3}}{2}-\frac{\sqrt{3}K_1}{2}+\frac{3K_3}{2} & \frac{3}{2}-\frac{\sqrt{3}K_2}{2}+\frac{3K_4}{2} \\ -\frac{\sqrt{3}}{2}+\frac{\sqrt{3}K_1}{2}+\frac{3K_3}{2} & \frac{3}{2}+\frac{\sqrt{3}K_2}{2}+\frac{3K_4}{2} \end{bmatrix} \cdot \begin{bmatrix} i_{\alpha s}{}^* \\ i_{\beta s}{}^* \end{bmatrix}$$

$$(25)$$

The relationship between the coefficients and the threshold derating factor can be obtained by iteratively varying the coefficients, based on (24) and (25). Fig. 3 shows the plot of a_o against K_1 and K_2, for the machine with two isolated neutrals. The coefficients and threshold derating factors that define different modes of post-fault operation with different neutral point configurations are summarized in Table I. Using the coefficients listed in Table I, the theoretical mean stator winding losses for different modes of post-fault operation can be calculated based on (22). The losses, normalised with respect to the stator winding loss of the healthy machine, are
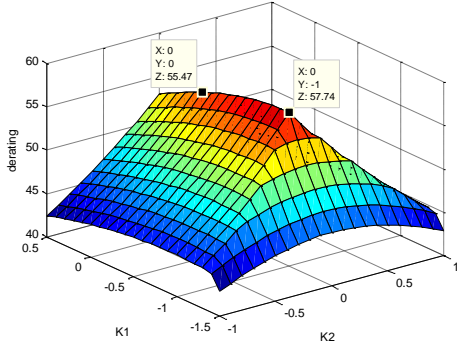

Fig. 3. Threshold derating factor (in %) as a function of K_1 and K_2, for asymmetrical six-phase induction machine with two isolated neutrals.

TABLE I. SUMMARY OF COEFFICIENTS FOR DIFFERENT MODES OF POST-FAULT OPERATION (OPEN-PHASE FAULT IN PHASE-C2)*

Neutrals	Mode	K_1	K_2	K_3	K_4	a_o
Two, isolated	Max Torque	-1	0	0	-1	0.577
	Min Loss	0	0	0	-1	0.555
Single, isolated	Max Torque	-0.295	-0.754	-0.209	-0.641	0.694
	Min Loss	0	0	0	-0.5	0.536

*Coefficients K_3 and K_4 are fixed (see (8)) for the machine with two isolated neutrals and this is indicated by using shaded cells.

TABLE II. NORMALISED MEAN STATOR WINDING LOSSES FOR DIFFERENT MODES OF POST-FAULT OPERATION

Neutrals	Mode	Mean Stator Losses (p.u.)
-	Single VSC	2.00
Two, isolated	Max Torque	2.00
	Min Loss	1.50
Single, isolated	Max Torque	1.73
	Min Loss	1.37

given in Table II. These losses are calculated assuming $a = 1$ (without derating); thus the losses can attain values up to twice the nominal value.

All the discussions and derivations so far were based on the open-circuit fault in phase-$c2$. Using the same principles, a set of machine equations that are similar to those presented in Section III can be obtained for fault in phase-$a1$. Instead of having coupling between β, y and 0- components, the coupling now exists between α, x and 0+ components.

Corresponding coefficients for post-fault operation can be obtained from Table I, by swapping β with α, y with x and 0- with 0+ components. The results are shown in Table III. Note that the result obtained for Max Torque mode of single isolated neutral case is identical to the one given in [22].

Due to the symmetry of the phases within each three-phase winding, the results in Table I and III can be made readily applicable to other phases by reordering the phase sequence. For fault that occurs in phase-$a1$, $b1$ or $c1$, post-fault strategy for phase-$a1$ can be adopted; for fault in phase-$a2$, $b2$ or $c2$, the strategy developed for phase-$c2$ can be used with corresponding phase rearrangement.

V. CONTROLLER FOR POST-FAULT OPERATION

In order to maintain the same controller structure for both healthy and faulted operation (as in Fig. 2), it is necessary to choose current controllers. For an n-phase machine, supplied using an n-leg VSC, the inverter's leg voltages and machine phase voltages are no longer related by a constant matrix during fault [11]. Instead, neutral point voltage of the stator winding is influenced by the back emf voltage of the faulted phase [15]. This introduces disturbance in the form of negative sequence voltage in α-β plane. To overcome this disturbance, dual PI controller is used for d-q current control during fault, as shown in Fig. 4. The negative sequence PI controller (dotted red box) is only activated during fault. For the x-y currents, since their references can be ac quantities, dual PI controller is used (Fig. 4) to enable effective regulation of the x-y currents.

From (9) and (11), it appears that, during the fault, there is an overlapping controller action for β, y and zero-sequence current controllers due to the coupling of the components. However this is not the case because connection of phase-$c2$ is lost during the fault, and v_{ys} (v_{0+s} and v_{0-s}, respectively) is no longer controllable by the VSC for the two (single) isolated neutrals case. To reflect the loss of the degree of freedom on control, y (zero-sequence, respectively) current controller is disabled during the fault for the two (single) isolated neutral case, by setting $v_{ys}{}^* = 0$ ($v_{0+s} = v_{0-s} = 0$). Note that the zero-sequence current controllers are only enabled during healthy operation of the machine with single neutral

TABLE III. SUMMARY OF COEFFICIENTS FOR DIFFERENT MODES OF POST-FAULT OPERATION (OPEN-PHASE FAULT IN PHASE-A1)*

Neutrals	Mode	K_1	K_2	K_3	K_4	a_o
Two, isolated	Max Torque	-1	0	0	-1	0.577
	Min Loss	-1	0	0	0	0.555
Single, isolated	Max Torque	-0.641	-0.209	-0.754	-0.295	0.694
	Min Loss	-0.5	0	0	0	0.536

*Coefficients K_1 and K_2 are fixed for the machine with two isolated neutrals and this is indicated by using shaded cells.
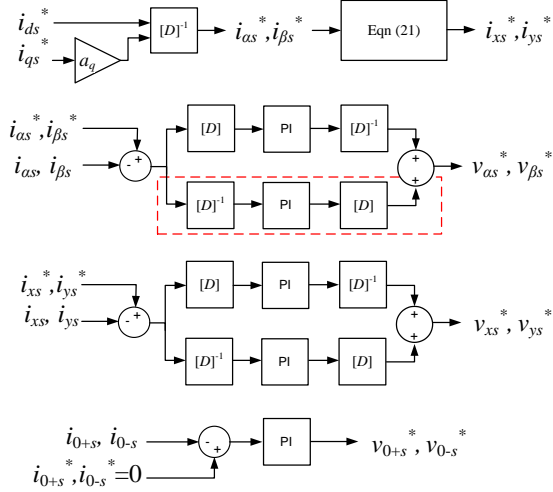
Fig. 4. Current controllers for control of a six-phase induction machine. Red dotted box shows the negative sequence PI controller which is only activated during fault.

TABLE IVI. EXPERIMENTAL SYSTEM PARAMETERS

Machine parameters			
$R_s = 12.5\ \Omega$	$R_r = 6.0\ \Omega$	$J = 0.04\ \text{kg·m}^2$	$p = 3$
$L_{ls\_dq} = 0.0615$ H	$L_{lr} = 0.011$ H	$L_m = 0.590$ H	
$L_{ls\_xy} = 0.0055$ H			
Converter Parameters			
$C = 1500\ \mu\text{F}$	$V_{dc} = 150$ V		
Controller Parameters			
d-q current controllers: $K_p = 60$	$K_i = 8000$		
x-y current controllers: $K_p = 50$	$K_i = 2500$		
Speed controller: $K_p = 0.02$	$K_i = 0.02$		

point connection.

As noted, the current control structure is shown in Fig. 4. The overall control structure remains unchanged and as in Fig. 2, with no modifications of the machine parameters or transformation matrix. Transition from healthy to post-fault operation involves enabling of the negative sequence PI current controllers in the *d-q* path, and disabling of *y* and/or zero-sequence current controllers depending on the neutral point configuration.

VI.   EXPERIMENTAL RESULTS

The experimental results were all obtained for the fault in phase-*c*2. The tests are conducted on a prototype six-pole asymmetrical six-phase induction machine, which is obtained by rewinding a 1.1 kW, 50 Hz three-phase machine. The machine is controlled in speed control mode with IRFOC. A dc machine, controlled using ABB DCS800 drive, is coupled to the six-phase machine and functions as a variable load. The machine, converter and control parameters used in the experiment are detailed in Table IV.

A six-leg VSC is used to control the six-phase machine. Switching frequency is selected as 2 kHz, and the currents are sampled at twice the switching frequency. Carrier-based pulse-width modulation is used, without any zero-sequence injection. The control is implemented using DS1006 dSpace

system with ControlDesk control environment. Experimental data, displayed in this section, are obtained by using the data capture function in ControlDesk and processed using Matlab. The results, presented here, focus only on the steady state behaviour of the machine under different modes of operation. The dynamic performance of the machine, including transition from healthy to faulted operation, is beyond the scope of this work.

A.   Healthy Operation

Fig. 5(a) shows the operation of the healthy asymmetrical six-phase machine when running at 250rpm with no load. Synchronous PI current controllers (only the positive sequence part) are used for *d-q* current regulation, while dual PI controllers are used for controlling the *x-y* currents, with $i_{xs}{}^* = i_{ys}{}^* = 0$. As seen from the figure, the phase currents are a balanced set of sinusoidal signals, while the α-β current space vector describes a circular trajectory. The *x-y* currents are controlled to zero to minimize losses. Under such healthy operation, the machine's speed is regulated at 250 rpm, with slight oscillations caused by the mechanical imperfections.

B.   Single Open-phase Fault

Single open-phase fault is emulated by removing the connection from VSC to phase-*c*2. Fig. 5(b) shows the corresponding operation of the machine without any modification to the current references and the controllers. Since $i_{ys}{}^*$ is still set to zero, the controller tries to minimize i_{ys}. This causes the disruption of the β current due to the coupling between stator *y* and β components. Instead of being regulated to the proper reference, β current is now almost zero. As a result of the improper control, the machine's speed shows significant oscillations.

Fig. 5(c) illustrates the case when the faulted machine operates with single active VSC. With connections to winding-*a*2*b*2*c*2 open-circuited, the machine is practically a three-phase machine with two degrees of freedom, and only α-β currents can be controlled. Hence, the *x-y* current controllers are disabled by setting $v_x{}^* = v_y{}^* = 0$. The α-β currents now track their references well, producing a circular trajectory that is the same as in the healthy case. The machine now operates with constant speed identical to that of the healthy machine. Even though this provides a simple means of post-fault control, the phase current amplitude in the remaining phases has now doubled. As will be shown later, better performance in terms of achievable torque and stator losses can be obtained using post-fault control strategies discussed in Section IV.

C.   Post-fault Operation (Two Isolated Neutrals)

Fig. 6 shows the post-fault operation of the machine, configured with two isolated neutrals. The α, β and *x* currents are now regulated with dual-PI controller, while *y* and zero-sequence current controllers are disabled ($v_{ys}{}^* = v_{0+s}{}^* = v_{0-s}{}^* = 0$). Figures 6(a) and (b) show the Min Loss and Max Torque modes of post-fault operation, respectively. For the Min Loss mode, the phase currents in the remaining five phases have unequal amplitudes. For the Max Torque mode, currents only flow in four of the remaining five phases, and all have the same amplitude. It can be observed that the maximum phase
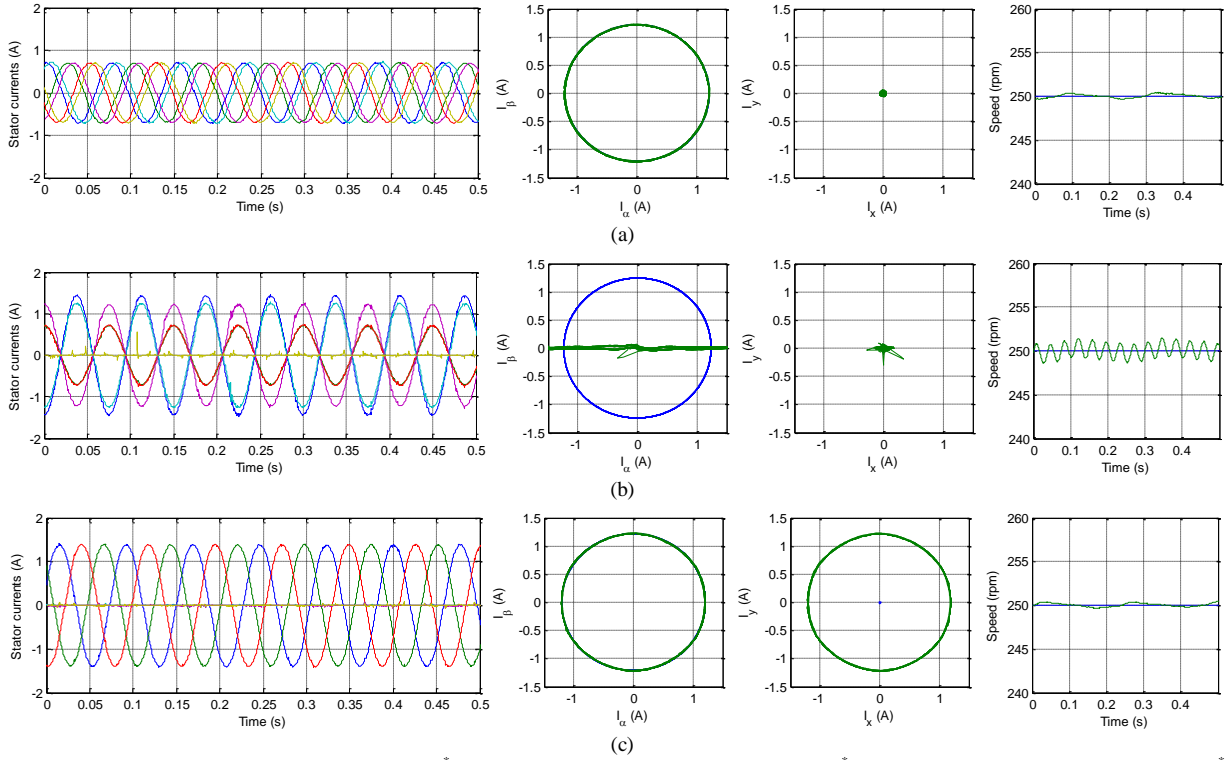
Fig. 5. Stator phase currents, α-β currents (blue trace=$i_{\alpha\beta}^*$; green trace= $i_{\alpha\beta}$), x-y currents (blue trace= i_{xy}^*, green trace= i_{xy}) and speed (blue trace=ω_m^*, green trace= ω_m) for (a) healthy machine and faulted machine (b) without modifications of current references ($i_x^* = i_y^* = 0$), (c) with 'single VSC' operation (winding-a2b2c2 disconnected). The machine is configured with two isolated neutrals and operates at 250 rpm without load..

current amplitude in Max Torque mode is slightly lower than that of the Min Loss mode, which is in agreement with the theoretical analysis in Section IV (regarding the values of a_o). Despite the difference in phase current waveforms, both modes of operation have their α-β currents well regulated to the references and the machine's speed remains practically constant, as in the healthy case. The maximum phase current amplitudes for both modes are also lower than in the 'single VSC' mode, suggesting a better performance.

D. Post-Fault Operation (Single Isolated Neutral)

Post-fault operation of the six-phase machine configured with single isolated neutral point is depicted in Fig. 7, with Figs. 7 (a) and 7 (b) showing Min Loss and Max Torque mode, respectively. The controller structure is the same as used for the two neutrals case. As discussed in Section V, all four α, β, x and y currents are controlled, so only zero-sequence current controllers are disabled ($v_{0+s}^* = v_{0-s}^* = 0$).

Similar to the two neutrals case, the α-β currents are well regulated under both modes and the machine runs at constant speed without obvious oscillations. For the Min Loss mode, the phase currents in the remaining five phases have different amplitudes, with the maximum phase current amplitude slightly higher than in the previous sub-section. On the other hand, operation in Max Torque mode yields phase currents of the same amplitude flowing in all the five remaining phases. The maximum phase current amplitude under this mode is found to be the lowest among all the discussed modes.

E. Derated Operation

So far, the results given in sub-sections A-D only show that different modes of post-fault operation can be achieved using the current references and controllers discussed in Sections IV and V. Next, the performance in different modes is compared in terms of the achievable torque and stator winding losses.

Fig. 8 shows the relationship between the normalized maximum phase current amplitude and the normalized torque, obtained based on (16), (19) and (20). With this plot, the achievable torque for different modes can be compared. As discussed earlier, the post-fault torque varies as the machine is derated. For 'single VSC' mode, the maximum achievable torque at rated phase current is found to be only approximately 43% of its rated value. As emphasized in Section IV, this depends on the ratio i_{dsn}/i_{qsn} of the machine, which in this case is 0.294. This is different from a six-phase permanent magnet machine, where 50% of the rated torque remains for 'single VSC' operation. Better performance can be obtained if the machine is controlled in Min Loss or Max Torque mode with two isolated neutrals, giving around 50% and 53%, respectively. The improvement provided by Max Torque is only marginal compared to Min Loss mode and the advantage in terms of additional torque can be easily outweighed by the increase in stator losses, as discussed shortly. Finally, the achievable torque is significantly improved, to approximately 66% of the rated value, when operating in Max Torque mode with single isolated neutral. The normalized stator losses of the faulted machine under different modes of operation are shown in Fig. 9. For each mode of operation, the phase currents of the machine under no-load condition are measured and transformed to the decoupled variables using transformation $[T_6]$. The stator winding losses are then
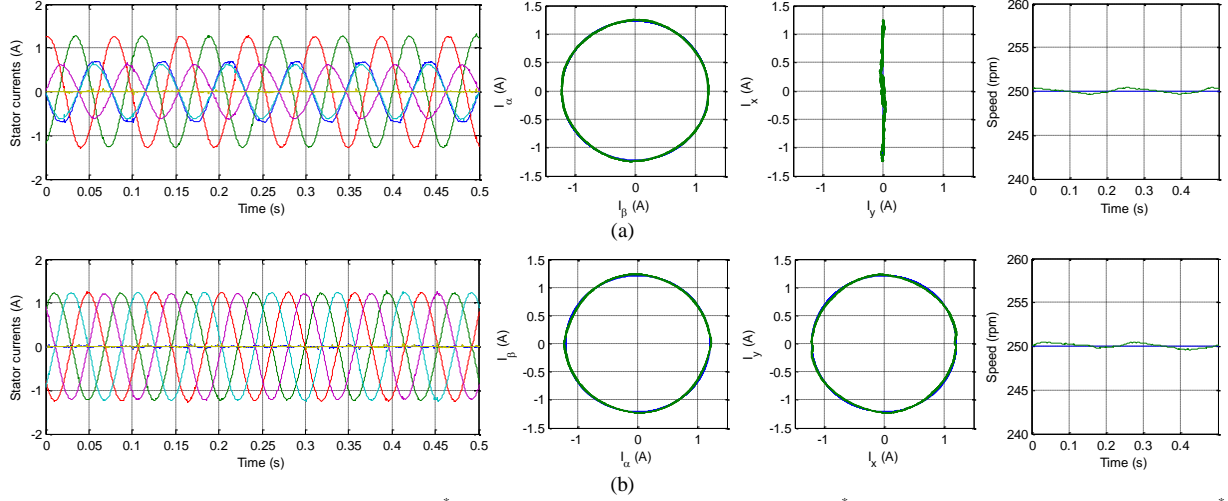
Fig. 6. Stator phase currents, α-β currents (blue trace=$i_{\alpha\beta}^*$; green trace= $i_{\alpha\beta}$), x-y currents (blue trace= i_{xy}^*, green trace= i_{xy}) and speed (blue trace=ω_m^*, green trace= ω_m) for faulted machine configured with two isolated neutrals, and controlled using (a) Min Loss and (b) Max Torque mode. The machine operates at 250 rpm without load

Fig. 7. Stator phase currents, α-β currents (blue trace=$i_{\alpha\beta}^*$; green trace= $i_{\alpha\beta}$), x-y currents (blue trace= i_{xy}^*, green trace= i_{xy}) and speed (blue trace=ω_m^*, green trace= ω_m) for faulted machine configured with single isolated neutral, and controlled using (a) Min Loss and (b) Max Torque mode. The machine operates at 250 rpm without load.
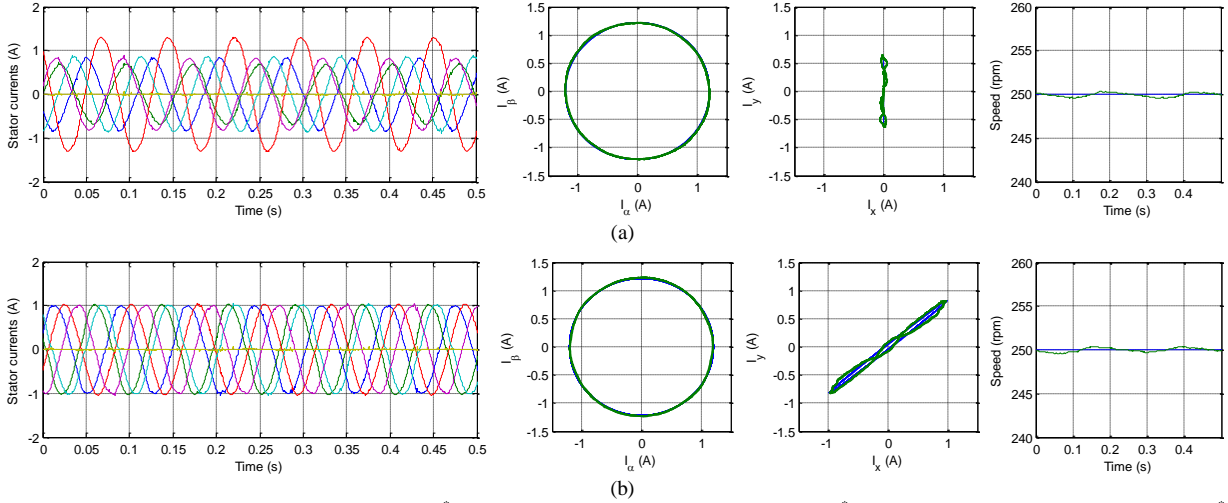
calculated based on (22) and normalized using the mean stator winding loss for healthy case. The experimental results (dotted lines) are in full accordance with the theoretical mean (solid lines) values shown in Table II. In terms of stator losses, Min Loss mode for the machine with single neutral gives the best performance. On the other hand, the Max Torque mode in configuration with two neutrals gives the worst performance, with mean stator winding losses being twice higher than for the healthy case. This is the same as operating the faulted machine in 'single VSC' mode. For the machine configured with two isolated neutrals, Min Loss mode gives lower stator winding loss, which is 25% lower than in the Max Torque mode. Considering that the difference of achievable torque between the two modes is small (only approximately 3%), Min Loss mode is more favourable mode of operation for the configuration with two neutrals.

Overall, the experimental results clearly show that, in an event of a fault, single isolated neutral configuration is significantly better than two isolated neutrals case, both in terms of achievable torque and stator loss minimization. Nevertheless, if configuration with two isolated neutrals is required, say, for safety or electrical isolation purposes, it is better to operate the machine under Min Loss mode.

VII. CONCLUSION

This paper analyzes post-fault operation of an asymmetrical six-phase induction machine, configured with single and two isolated neutrals. Using the same decoupling transformation, the effects of a single open-phase fault on the machine equations are addressed. It is pointed out that the fault only affects the mutual relationship between axis current components, so that the same machine equations, based on healthy decoupling transformation [T_6], can still be used for post-fault control. Regardless of the neutral point connection, the same controller structure can still be used, with only minor modifications of current references and the enabling/disabling of the controllers.
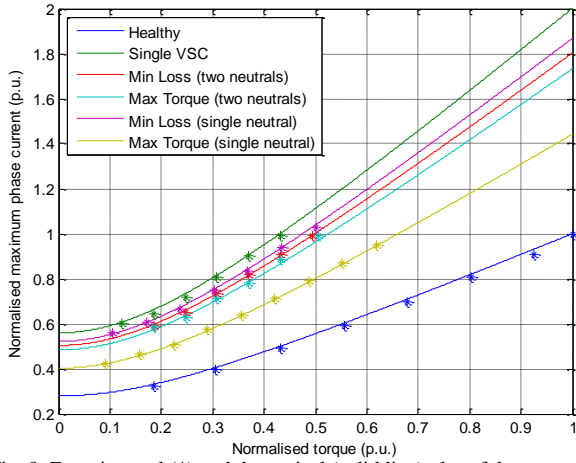
Based on the decoupling transformation [T_6], and the

Fig. 8. Experimental (*) and theoretical (solid line) plot of the normalized maximum phase current against normalized torque for the asymmetrical six-phase induction machine operating under different post-fault operation modes ($i_{dsn}/i_{qsn} = 0.294$).
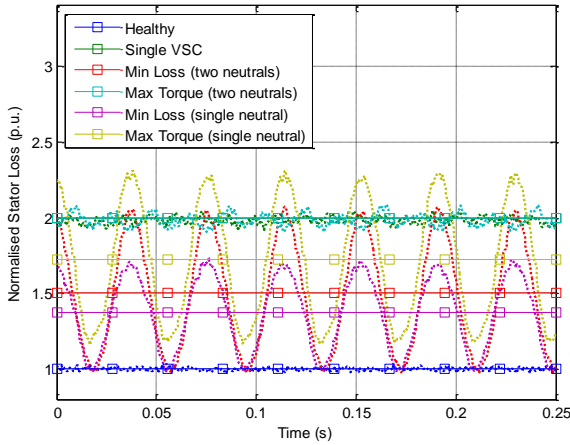

Fig. 9. Instantaneous (dotted lines) and theoretical mean (solid lines) of the normalised stator winding losses, for healthy and faulted asymmetrical six-phase induction machine under different modes of post-fault operation (the theoretical means for 'single VSC' and Max Torque (two neutrals) overlap).

current component inter-dependencies during the fault, different modes of post-fault operation have been analyzed. The performance of these different modes of control, in terms of achievable torque and stator losses, has been compared, with an overall conclusion that better post-fault behaviour results for the single isolated neutral configuration.

REFERENCES

[1] E. Levi, "Multiphase electric machines for variable-speed applications," *IEEE Trans. on Industrial Electronics*, vol. 55, no. 5, pp. 1893–1909, 2008.

[2] L. Alberti and N. Bianchi, "Experimental tests of dual three-phase induction motor under faulty operating condition," *IEEE Trans. on Industrial Electronics*, vol. 59, no. 5, pp. 2041–2048, 2012.

[3] M. Barcaro, N. Bianchi, and F. Magnussen, "Analysis and tests of a dual three-phase 12-slot 10-pole permanent magnet motor," *IEEE Trans. on Industrial Applications*, vol. 46, no. 6, pp. 2355–2362, Sep. 2010.

[4] E. Semail, X. Kestelyn, and F. Locment, "Fault tolerant multiphase electrical drives: the impact of design," *The European Physical Journal − Applied Physics*, vol. 43, no. 2, pp. 159–163, 2008.

[5] N. Bianchi, S. Bolognani, and M. D. Pré, "Impact of stator winding of a five-phase permanent-magnet motor on postfault operations," *IEEE Trans. on Industrial Electronics*, vol. 55, no. 5, pp. 1978–1987, 2008.

[6] B. Vaseghi, N. Takorabet, J. P. Caron, B. Nahid-mobarakeh, F. Meibody-Tabar, and G. Humbert, "Study of different architectures of fault-tolerant actuator using a two-channel PM motor," *IEEE Trans. on Industry Applications*, vol. 47, no. 1, pp. 47–54, 2011.

[7] M. A. Parker, C. Ng, and L. Ran, "Fault-tolerant control for a modular generator−converter scheme for direct-drive wind turbines," *IEEE Trans. on Industrial Electronics*, vol. 58, no. 1, pp. 305–315, Jan. 2011.

[8] M. A. Parker, L. Ran, and S. J. Finney, "Distributed control of a fault-tolerant modular inverter for direct-drive wind turbine grid interfacing," *IEEE Trans. on Industrial Electronics*, vol. 60, no. 2, pp. 509–522, 2013.

[9] G. Grandi, P. Sanjeevikumar, Y. Gritli, and F. Filippetti, "Fault-tolerant control strategies for quad inverter induction motor drives with one failed inverter," *Int. Conf. on Electrical Machines ICEM*, Marseille, France, 2012, pp. 959–966.

[10] M. Ruba and D. Fodorean, "Analysis of fault-tolerant multiphase power converter for a nine-phase permanent magnet synchronous machine," *IEEE Trans. on Industry Application*, vol. 48, no. 6, 2012, pp. 2092–2101.

[11] Y. Zhao and T. A. Lipo, "Modeling and control of a multi-phase induction machine with structural unbalance - Part I. Machine modeling and multi-dimensional current regulation," *IEEE Trans. on Energy Conversion*, vol. 11, no. 3, pp. 570–577, 1996.

[12] Y. Zhao and T. A. Lipo, "Modeling and control of a multi-phase induction machine with structural unbalance - Part II. Field-oriented control and experimental verification," *IEEE Trans. on Energy Conversion*, vol. 11, no. 3, pp. 578–584, 1996.

[13] R. Kianinezhad, B. Nahid-Mobarakeh, L. Baghli, F. Betin, and G.-A. Capolino, "Modeling and Control of Six-Phase Symmetrical Induction Machine Under Fault Condition Due to Open Phases," *IEEE Trans. on Industrial Electronics*, vol. 55, no. 5, pp. 1966–1977, May. 2008.

[14] H. Ryu, J. Kim, and S. Sul, "Synchronous-Frame Current Control of Multiphase Synchronous Motor Under Asymmetric Fault Condition Due to Open Phases," *IEEE Trans. on Industrial Applications*, vol. 42, no. 4, pp. 1062–1070, 2006.

[15] H. Guzmán, M. J. Durán, F. Barrero, and S. Toral, "Fault-tolerant current predictive control of five-phase induction motor drives with an open phase," in *IECON 2011 - 37th Annual Conference of the IEEE Industrial Electronics Society*, 2011, pp. 3680–3685.

[16] F. Locment, E. Semail, and X. Kestelyn, "Vectorial approach-based control of a seven-phase axial flux machine designed for fault operation," *IEEE Trans. on Industrial Electronics*, vol. 55, no. 10, pp. 3682–3691, Oct. 2008.

[17] L. Parsa and H. A. Toliyat, "Fault-tolerant interior-permanent-magnet machines for hybrid electric vehicle applications," *IEEE Trans. on Vehicular Technology*, vol. 56, no. 4, pp. 1546–1552, 2007.

[18] S. Dwari and L. Parsa, "An optimal control technique for multiphase PM machines under open-circuit faults," *IEEE Trans. on Industrial Electronics*, vol. 55, no. 5, pp. 1988–1995, May. 2008.

[19] S. Dwari and L. Parsa, "Fault-tolerant control of five-phase permanent-magnet motors with trapezoidal back EMF," *IEEE Trans. on Industrial Electronics*, vol. 58, no. 2, pp. 476–485, Feb. 2011.

[20] F. Baudart, B. Dehez, E. Matagne, D. Telteu-Nedelcu, P. Alexandre, and F. Labrique, "Torque control strategy of polyphase permanent-magnet synchronous machines with minimal controller reconfiguration under open-circuit fault of one phase," *IEEE Trans. on Industrial Electronics*, vol. 59, no. 6, pp. 2632–2644, 2012.

[21] A. Tani, M. Mengoni, L. Zarri, G. Serra, and D. Casadei, "Control of multiphase induction motors with an odd number of phases under open-circuit phase faults," *IEEE Trans. on Power Electronics*, vol. 27, no. 2, pp. 565–577, 2012.

[22] J.-R. Fu and T. A. Lipo, "Disturbance-free operation of a multiphase current-regulated motor drive with an opened phase," *IEEE Trans. on Industry Applications*, vol. 30, no. 5, pp. 1267–1274, 1994.

[23] C. B. Jacobina, R. S. Miranda, M. B. R. C. De, and S. Luis, "Disturbance-free operation of a six-phase AC motor drive system," *IEEE Power Electronics Specialists Conf. PESC*, Aachen, Germany, 2004, no. 3, pp. 925–931.

[24] M.-A. Shamsi-Nejad, B. Nahid-Mobarakeh, S. Pierfederici, and F. Meibody-Tabar, "Fault tolerant and minimum loss control of double-star synchronous machines under open phase conditions," *IEEE Trans. on Industrial Electronics*, vol. 55, no. 5, pp. 1956–1965, May. 2008.

[25] F. Lin, Y. Hung, J. Hwang, and M. Tsai, "Fault-tolerant control of a six-phase motor drive system using a Takagi-Sugeno-Kang type fuzzy neural network with asymmetric membership function," *IEEE Trans. on Power Electronics*, vol. 28, no. 7, pp. 3557–3572, 2013.

[26] A. Mohammadpour and L. Parsa, "A unified fault-tolerant current control approach for five-phase PM motors with trapezoidal back EMF under different stator winding connections," *IEEE Trans. on Power Electronics*, vol. 28, no. 7, pp. 3517–3527, Jul. 2013.

[27] M. A. Fnaiech, F. Betin, G.-A. Capolino, and F. Fnaiech, "Fuzzy logic and sliding-mode controls applied to six-phase induction machine with open phases," *IEEE Trans. on Industrial Electronics*, vol. 57, no. 1, pp. 354–364, Jan. 2010.

[28] J. W. Bennett, B. C. Mecrow, D. J. Atkinson, and G. J. Atkinson, "Safety-critical design of electromechanical actuation systems in commercial aircraft," *IET Electric Power Applications*, vol. 5, no. 1, pp. 37–47, 2011.

[29] E. Jung, H. Yoo, S.-K. Sul, H.-S. Choi, and Y.-Y. Choi, "A nine-phase permanent-magnet motor drive system for an ultrahigh-speed elevator," *IEEE Trans. on Industry Applications*, vol. 48, no. 3, pp. 987–995, 2012.

Hang Seng Che received his BEng degree in Electrical Engineering from the University of Malaya, Malaysia, in 2009. He then obtained his PhD degree in 2013 under auspices of a dual PhD programme between the University of Malaya and Liverpool John Moores University, Liverpool, UK. He is currently working as a postdoctoral research fellow in Power Energy Dedicated Advanced Center (UMPEDAC), University of Malaya, Malaysia. Dr. Che was the recipient of the 2009 Kuok Foundation Postgraduate Scholarship Award for his PhD study. His research interests include multiphase machines, fault tolerant control and renewable energy.

Mario J. Duran was born in Malaga, Spain, in 1975. He received the M.Sc. and Ph.D. degrees in Electrical Engineering from the University of Malaga, Spain, in 1999 and 2003, respectively. He is currently an Associate Professor with the Department of Electrical Engineering at the University of Málaga. Mario is the recipient of the Best Paper Award from the IEEE Transactions on Industrial Electronics in 2009. His research interests include modeling and control of multiphase drives and renewable energy conversion systems.

Emil Levi (S'89, M'92, SM'99, F'09) received his M.Sc. and PhD degrees from the University of Belgrade, Yugoslavia in 1986 and 1990, respectively. From 1982 till 1992 he was with the Dept. of Elec. Engineering, University of Novi Sad. He joined Liverpool John Moores University, UK in May 1992 and is since September 2000 Professor of Electric Machines and Drives. He serves as Co-Editor-in-Chief of the IEEE Trans. on Industrial Electronics, as an Editor of the IEEE Trans. on Energy Conversion, and as Editor-in-Chief of the IET Electric Power Applications. Emil is the recipient of the Cyril Veinott award of the IEEE Power and Energy Society for 2009.

Martin Jones received his BEng degree (First Class Honours) in Electrical Engineering from the Liverpool John Moores University, UK in 2001. He was a research student at the Liverpool John Moores University from September 2001 till Spring 2005, when he received his PhD degree. Dr Jones was a recipient of the IEE Robinson Research Scholarship for his PhD studies and is currently with Liverpool John Moores University as a Reader. His research is in the area of high performance ac drives.

Wooi-Ping Hew (M'06) obtained his BEng and Masters (Electrical) degrees from the University of Technology, Malaysia. He received his PhD from the University of Malaya, Kuala Lumpur, Malaysia in 2000. He is currently a Professor in the Faculty of Engineering, University of Malaya, Kuala Lumpur, Malaysia. Dr. Hew is a Member of IET and a Chartered Engineer. His research interests include electrical drives and electrical machine design.

Nasrudin A. Rahim (M'89, SM'08) received the B.Sc. (Hons.) and M.Sc. degrees from the University of Strathclyde, Glasgow, U.K., and the PhD degree from Heriot–Watt University, Edinburgh, U.K., in 1995. He is currently a Professor with the Faculty of Engineering, University of Malaya, Kuala Lumpur, Malaysia, where he is also the Director of the Power Energy Dedicated Advanced Center (UMPEDAC). Prof. Rahim is a Fellow of the IET, U.K., and the Academy of Sciences Malaysia.